CCI+ PHASE 2
PERMAFROST

CCN4 OPTION 7
ICEINSAR: INFERRED ACTIVE LAYER WATER/ICE CONTENT AND FREEZE-THAW PROGRESSION FROM ASSIMILATING INSAR IN PERMAFROST MODEL

D1.2 PRODUCT SPECIFICATION DOCUMENT (PSD)

VERSION 1.0

31 MARS 2023

PREPARED BY

Document Status Sheet

Issue	Date	Details	Authors
0.1	20.03.2023	Template based on baseline URD	L. Rouyet (NORCE)
0.2	27.03.2023	First draft CCN4 Option 7 D1.1	L. Rouyet, L. Wendt (NORCE)
0.3	29.03.2023	Updated/corrected version CCN4 Option 7 D1.1	S. Westermann (UiO), A. Bartsch (B.GEOS), Strozzi (GAMMA)
1.0	31.03.2023	Final version CCN4 Option 7 D1.1	L. Rouyet (NORCE), L. Wendt (NORCE), S. Westermann (UiO), A. Bartsch (B.GEOS), Strozzi (GAMMA)

Author team

Line Rouyet and Lotte Wendt, NORCE

Sebastian Westermann, UiO

Annett Bartsch, B.GEOS

Tazio Strozzi, GAMMA

ESA Technical Officer

Frank Martin Seifert

TABLE OF CONTENTS

EXECUTIVE SUMMARY

Within the European Space Agency (ESA), the Climate Change Initiative (CCI) is a global monitoring program which aims to provide long-term satellite-based products to serve the climate modelling and climate user community. The two main products associated to the ECV Permafrost are Ground Temperature (GT) and Active Layer Thickness (ALT). GT and ALT are documented by the Permafrost_cci project based on thermal remote sensing and physical modelling.

The Permafrost_cci models take advantage of additional datasets, such as snow cover and land cover, to estimate the heat transfer between the surface and the underground. However, several challenges remain due to spatially variable subsurface conditions, especially in relation to unknown amounts of water/ice in the active layer that modify the effective heat capacity and the thermal conductivity of the ground. In complex terrain with large spatial heterogeneities, coarse and partly inadequate land cover categorisation, the current results show discrepancies with in-situ measurements, which highlight the need to assimilate new data sources as model input. Although the ground stratigraphy is not directly observable from space, it impacts the dynamics of the ground surface. The seasonal thawing and refreezing induce cyclic subsidence and heave of the ground surface due to ice formation and melt in the active layer, and can therefore be used as indirect indicator of the ground conditions.

Synthetic Aperture Radar Interferometry (InSAR) based on Sentinel-1 images can be used to measure the amplitude and seasonal progression of these displacements. The movement amplitude is related to the amount of water/ice that is affected by a phase change, whilst the timing of the displacement patterns reflects the vertical progression of the thawing/freezing front. Considering the fine to medium spatial resolution of Sentinel-1 images, InSAR time series therefore have the potential to enhance the characterisation of subsurface hydrogeologic and thermal parameters and adapt the existing Permafrost_cci models to improve their performance at the local to regional scale. The *IceInSAR* pilot project (Option 7) will develop a prototype for permafrost model adjustment by assimilating Sentinel-1 InSAR surface displacement maps and time series into the model to constrain stratigraphy parameters. *IceInSAR* will provide pilot products, expected to be used for adjustment of the ECV processing chain of the baseline project in a next phase.

This Product Specification Document (PSD) describes the properties of the Svalbard study areas and products that will be generated by the *IceInSAR* Option 7, following the targeted user requirements identified in URD for Option 7 (RD-1). The project considers the traditional Permafrost_cci products, the ground temperature at a certain depth (GTD) and the active layer thickness (ALT), as well as an additional product, the InSAR-based surface displacements (SD). For SD, this PSD defines two products: the seasonal SD time series (SSD) and the multi-seasonal SD maps (MSD). For the traditional Permafrost_cci parameters, this PSD considers the priorities established by the baseline project (RD-2), while adjusting the specifications to the specific scope and objective of the Option 7. After assimilation of InSAR-based SD in the model, we aim to deliver GTD and ALT at a higher spatio-temporal resolution and an expected higher product accuracy. The final spatial coverage of the Option 7 pilot products is however much smaller: at the local scale (at selected locations with available in-situ measurements) and at the regional scale (flat lowlands in three study areas of Spitsbergen, Svalbard).

1 INTRODUCTION

1.1 Purpose of the document

This document describes the product specifications in order to obtain a permafrost product that is consistent, stable and error-characterised. The purpose of this document is to present the structure, syntax and file naming conventions used to describe the different permafrost products generated in the *IceInSAR* Option 7. It provides all the necessary data needed by permafrost algorithm developers and users to respectively write and read the permafrost products.

1.2 Structure of the document

Section 2 describes the area covered for the service as well as regions of interest for evaluation. The remaining sections detail the product specifications (Section 3) and format (Section 4). A bibliography complementing the applicable and reference documents (Sections 1.3 and 1.4) is provided in Section 5.1. A list of acronyms is provided in Section 5.2. A glossary of the commonly accepted permafrost terminology can be found in [RD-9].

1.3 Applicable documents

[AD-1] ESA. 2022. Climate Change Initiative Extension (CCI+) Phase 2 – New Essential Climate Variables – Statement of Work. ESA-EOP-SC-AMT-2021-27.

[AD-2] GCOS. 2022. The 2022 GCOS Implementation Plan. GCOS – 244 / GOOS – 272. Global Observing Climate System (GCOS). World Meteorological Organization (WMO).

[AD-3] GCOS. 2022. The 2022 GCOS ECVs Requirements. GCOS – 245. Global Climate Observing System (GCOS). World Meteorological Organization (WMO).

1.4 Reference Documents

[RD-1] Rouyet, L., Wendt, L., Westermann, S., Bartsch, A., Strozzi, T. 2023. ESA CCI+ Permafrost Phase 2. CCN4 Option 7. IceInSAR: Inferred Active Layer Water/Ice Content and Freeze-Thaw Progession From Assimilating InSAR in Permafrost Model. D.1.1 User Requirement Document (URD). Version 1.0. European Space Agency.

[RD-2] Bartsch, A., Westermann, S., Strozzi, T., Wiesmann, A., Kroisleitner, C., Wieczorek, M., Heim, B. 2023. ESA CCI+ Permafrost Phase 2. D1.2 Product Specification Document (PSD). Version 3.0. European Space Agency.

[RD-3] Heim, B., Wieczorek, M., Pellet, C., Barboux, C., Delaloye, R., Bartsch, A., Strozzi, T. (2019): ESA CCI+ Product validation and intercomparison report (PVIR), v1.0

[RD-4] Heim, B., Wieczorek, M., Pellet, C., Delaloye, R., Bartsch, A., Strozzi, T. (2020): ESA CCI+ D.4.1 Product validation and intercomparison report (PVIR), v2.0

[RD-5] Heim, B., Lisovski, S., Wieczorek, M., Pellet, C., Delaloye, R., Bartsch, A., Jakober, D., Pointer, G., Strozzi, T. (2021): ESA CCI+ D.4.1 Product validation and intercomparison report (PVIR), v3.0

[RD-6] Duchossois G., P. Strobl, V. Toumazou, S. Antunes, A. Bartsch, T. Diehl, F. Dinessen, P. Eriksson, G. Garric, M-N. Houssais, M. Jindrova, J. Muñoz-Sabater, T. Nagler, O. Nordbeck. 2018. User Requirements for a Copernicus Polar Mission - Phase 1 Report, EUR 29144 EN, Publications Office of the European Union, Luxembourg, 2018, ISBN 978-92-79-80961-3, https://doi.org/10.2760/22832, JRC111067.

[RD-7] National Research Council. 2014. Opportunities to Use Remote Sensing in Understanding Permafrost and Related Ecological Characteristics: Report of a Workshop. Washington, DC: The National Academies Press. https://doi.org/10.17226/18711.

[RD-8] Bartsch, A., G. Hugelius, Strozzi, T. 2021. ESA CCI+ Permafrost CCN3 Option 6: improved soil description through a landcover map dedicated for the Arctic. User Requirements Document, v1.0.

[RD-9] van Everdingen, Robert, Ed. 1998 revised May 2005. Multi-language glossary of permafrost and related ground-ice terms. Boulder, CO: National Snow and Ice Data Center/World Data Center for Glaciology. (http://nsidc.org/fgdc/glossary/; accessed 23.09.2009).

1.5 Bibliography

A complete bibliographic list that supports arguments or statements made within the current document is provided in Section 5.1.

1.6 Acronyms

A list of acronyms is provided in Section 5.2.

2 KEY REGIONS FOR STUDY

The *IceInSAR* Option 7 focuses on the flat lowlands within three study areas of Spitsbergen, Svalbard: Adventdalen (ADV), Kapp Linné (KL) and Ny-Ålesund (NYA) (Fig.1). Svalbard is characterized by a polar-tundra climate (Peel et al., 2007) with permafrost at all elevations of the glacier-free areas. The island of Spitsbergen experiences a large climatic gradient with higher temperature and greater precipitation in the west influenced by mild oceanic currents, compared to the more continental interior (Hanssen-Bauer et al., 2019). The seasonal and interannual meteorological variations, the variable topography combining high mountains, large sediment-infilled valleys and strandflats, as well as the diversity of the local environmental conditions lead to large spatio-temporal heterogeneities of the ground thermal regime. The complex setting makes the region ideal to test the effect of constraining and increasing the resolution of the Permafrost_cci products using InSAR-based surface displacements. In addition, the global Permafrost_cci products show a general bias towards high ground temperature and thick active layer, expected to be related to the simplistic and coarse landcover categorization being unable to represent the complexity of the ground properties in Svalbard (PVIR 1.0, 2.0 and 3.0 [RD-3] [RD-4] [RD-5]). The attempt to use InSAR maps to enhance the characterization of subsurface hydrogeologic and thermal parameters and improve the model performance at the regional scale is therefore especially relevant for Svalbard.

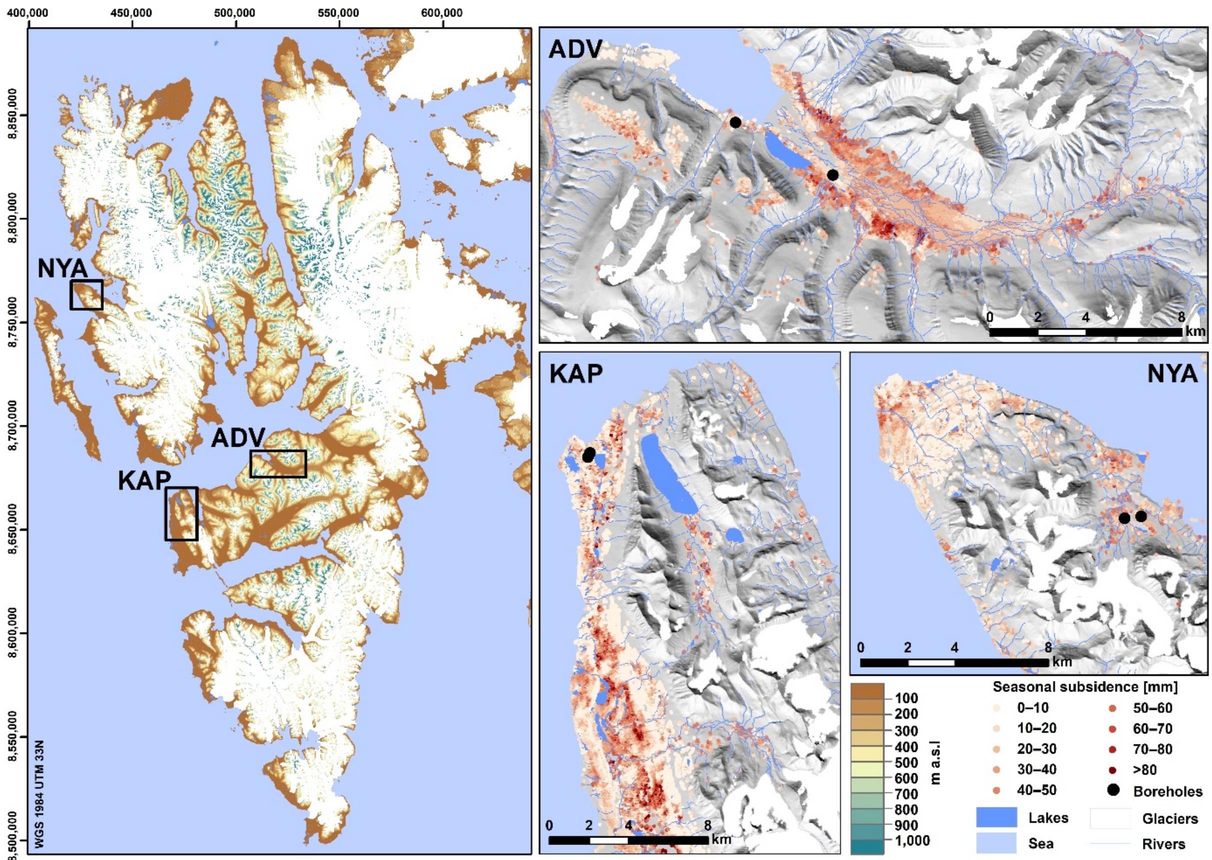

Figure 1: Study areas in Adventdalen (ADV), Kapp Linné (KAP) and Ny-Ålesund (NYA). The *IceInSAR* Option 7 focuses on the flat lowlands within these areas (valley bottoms, strandflats). In the insets on the right: see examples of data coverage from previously processed InSAR subsidence maps based on 2017 Sentinel-1 images. The black dots show the locations of the main available permafrost monitoring boreholes (Christiansen et al., 2021). Modified from Rouyet et al. (2021).

2.1 Adventdalen (ADV)

Adventdalen is a SE–NW oriented valley tributary to the Isfjord system. Longyearbyen, the main Svalbard's settlement is located in the western part of the study area (Fig.1). The Adventdalen (ADV) study area has complex topography with mountain tops up to approx. 1050 m a.s.l. and valleys down to the sea level, carved into sedimentary rocks (primarily sandstones and shales) (Major et al., 2001). Following regional deglaciation, fluvial and periglacial processes have further developed the ADV geomorphology. The valley flows are infilled by variably distributed fluvial, alluvial and eolian sediments with contrasting properties, grain sizes and frost-susceptibilities (Tolgensbakk et al., 2001). Ground ice distribution is also highly variable, with higher contents observed in the top few meters of syngenetic permafrost, especially in eolian deposits, and at the top of underlying epigenetic permafrost (Gilbert et al., 2018; Cable et al., 2018). In 2017–2019, the mean annual temperature at the permafrost surface (upper-most sensor in the permafrost) varied between approx. -2 and -4 °C in the two main Svalbard Integrated Observing System (SIOS) boreholes of the lower Adventdalen. The ALT was approx. between 75 and 125 cm (Christiansen et al., 2021). The active layer generally thaws between approx. June and September, although the duration of the thawing period varies from year to year. Previous studies show that InSAR maps are well able to document the spatial variability of the seasonal displacement amplitude, related with the distribution of various landform and surficial material types (Rouyet et al., 2019), while InSAR subsidence-heave time series reflect the seasonal progression of the thawing and freezing in the active layer (Rouyet et al., 2021).

2.2 Ny-Ålesund (NYA)

The Ny-Ålesund (NYA) study area is located along Kongfjorden in northwestern Spitsbergen and includes a large research station converted from a former coal mining village (Fig.1). NYA is characterized by a strandflat in the western part of the Brøggerhalvøya peninsula and steep topography with peaks at 790 m a,s,l, in the southern part. The sedimentary bedrock is covered by a large variety of terrestrial and coastal sediments (till, colluvial, fluvial and raised beach deposits) (Hjelle, 1999; Miccadei, et al., 2016). Fine-scale variabilities of surface conditions (e.g. snow cover) and ground properties have been reported in the well-studied Bayelva area and influence the way the air temperature transfers into the ground (Boike et al., 2003; Westermann et al., 2010; 2011). At this location, a permafrost research sites collects long-term environmental data since 1998 (Boike et al., 2018). In 2017–2019, the mean annual temperature at the permafrost surface (upper-most sensor in the permafrost) varied between approx. -2.5 and -3.5 °C in the two main boreholes of the Svalbard Integrated Observing System (SIOS). The ALT was approx. between 150 and 200 cm (Christiansen et al., 2021). Previous analyses of InSAR-based displacement time series from active layer seasonal freeze and thaw progression have also been performed in the NYA study area (Rouyet et al., 2021).

2.2 Kapp Linné (KL)

The Kapp Linné (KL) study area is located in the westernmost part of the Nordenskiöld peninsula (Fig.1). Influenced by the North Atlantic maritime regime, this is one of the warmest parts of Spitsbergen (Retelle et al., 2020). The Isfjord Radio weather station, used as research facility for field operations, is situated in the northwestern part, close to the shore. The area is characterized by a low-lying Precambrian bedrock platform – the strandflat – mantled by raised beach deposits (Landvik et al., 1987). The strandflat consists of a complex assemblage of dry, coarse-grained, raised marine beach ridges and exposed weathered bedrock, interspersed with thermokarst lakes, organic-rich shallow bogs with a large variety of permafrost landforms (small palsas, ice-wedge polygons, sorted/unsorted circles) (Åkerman, 2005; Eckerstorfer et al., 2017). Further west, the Griegfjellet ridgeline leads to a dramatic change of topography, with peaks reaching up to approx. 780 m a.s.l. Close to Isfjord Radio, permafrost observations have been carried out since 2008 (Christiansen et al., 2010). In 2017–2019, the mean annual temperature at the permafrost surface (upper-most sensor in the permafrost) varied between approx. -1.5 and -2.5 °C in the two main boreholes of the Svalbard Integrated Observing System (SIOS). The ALT was approx. between 175 and 300 cm (Christiansen et al., 2021). Analyses of InSAR-based displacement time series from active layer seasonal freeze and thaw progression have also been performed in the KL study area (Rouyet et al., 2021).

3 PRODUCTS SPECIFICATIONS

3.1 Surface displacement (SD)

3.1.1 Product description

This product consists of maps and time series documenting the distribution and seasonal progression of the freeze/thaw-related surface displacements (SD) based on Sentinel-1 Synthetic Aperture Radar Interferometry (InSAR). Sloping terrain will be discarded to focus on flat lowlands assumed to be dominated by vertical SD (i.e. strandflats and sediment-infilled valley bottoms). Initial line-of-sight (LOS) SD will therefore be projected vertically. We will provide **two types of complementary SD products** to test the InSAR assimilation into the Permafrost_cci model:

- **Seasonal SD time series (SSD):** Image pairs (interferograms) will be generated within snow-free seasons (May–June to October–November) in 2017–2021 based on Sentinel-1 Interferometric Wide (IW) swath images with a time interval (temporal baseline) depending on the coherence variability during the observation window. To minimise the processing steps required for product generation before assimilation in the model, we will test the feasibility of using single wrapped (cyclic phase) and unwrapped (absolute phase) interferograms as model inputs. However, single interferograms are expected to have a low signal-to-noise ratio due to the impact of unwanted phase components, such as the Atmospheric Phase Screen (APS) (Hanssen, 2001). We will therefore also process the 2017–2021 seasonal SD time series with the multi-temporal Small BAseline Subset (SBAS) algorithm (Berardino et al., 2002), which uses the redundancy of overlapping interferograms to mitigate the atmospheric component. Previous work has evidenced that SBAS time series can document fine temporal variability of subsidence and heave patterns, able to reflect the seasonal progression of thawing and freezing front in the active layer (Rouyet et al., 2019). The time series can be used to identify late-summer secondary subsidence patterns highlighting degradation of ice-rich layers at the top of the permafrost (Bartsch et al. 2019, Zwieback & Meyer, 2021). Based on the SBAS time series, we will generate SD maps showing the maximal displacement of each snow-free season. These maps are used to document the spatio-temporal variability of the active layer water/ice content for each season.
- **Multi-seasonal SD maps (MSD):** The multi-seasonal product is an averaged SD map discarding information regarding the inter-seasonal variability of the signal to focus on the spatial patterns only. The SD amplitude in permafrost environment is highly related to the frost-susceptibility of the ground material, i.e. the ability for water to turn into ice lenses and lift up the ground surface during the freezing period. As frost-susceptibility depends on the material grain size, there is a relationship between the seasonal movement amplitude and the landcover type (Bartsch et al., 2019) or geomorphological units (Rouyet et al., 2019), which will be used to generate InSAR-based geocryological maps to constrain the parametrization of the ground stratigraphy in the model.

The products will be generated for the three study areas (ADV, NYA and KL) described in Section 2.

3.1.2 Temporal resolution

The temporal resolution of the SD time series will correspond to the repeat-pass of Sentinel-1, i.e. 6-days for the seasons when both Sentinel-1A and -1B images were available (2017–2021). Due to coherence loss during the winter, this applies to the snow-free periods only, which have variable durations depending on the year and the study area (typically May–June to October–November in Svalbard).

3.1.3 Spatial resolution

The initial resolution of Sentinel-1 IW images is approx. 5 m in range and 20 m in azimuth. Complex spatial averaging (multi-looking) improves the signal stability and dampens the influence of unrepresentative scattering effects within resolution cells. We will evaluate these effects by testing different InSAR multi-looking factors, which will lead to a final ground resolution between 40–100 m. It should also be noted that the InSAR information will be spatially discontinuous. Areas affected by typical SAR geometrical limitations (shadow/layover) and interferometric coherence loss due to wet/snow-covered surfaces or fast displacements (> ¼ the wavelength during the time interval of the interferograms, i.e. about 1.4 cm in 6 days) will remain undocumented.

3.1.4 Product accuracy

For SD, the JRC report on User Requirements for a Copernicus Polar Mission [RD-6] requires a vertical accuracy of 0.001 m/yr (goal) to 0.01 m/yr (threshold) (see URq_20 in the URD [RD-1]).

In the *IceInSAR* Option 7, despite the relatively short temporal baseline (intra-seasonal) and the short time observation window of the SBAS (approx. 0.5 year), the accuracy is estimated to be above the threshold requirement (0.01 m/yr). This is due to the small extent of the study areas (i.e. short distances to the reference point), as well as the frequent repeat-pass of Sentinel-1 resulting in a large number of interferograms (see Eq. 19, Emardson et al., 2003). The standard deviation of the retrieved velocity depends on the number of interferograms (60–100 per season) and the temporal baseline (6–48d depending on the time period). Assuming a standard deviation of 5 mm per interferogram due to the atmosphere, the standard deviation is estimated to go down to a few mm (1–3 mm) for seasons with 6-days repeat-pass (2017–2021) (see Eq. 11, Emardson et al., 2003).

Considering the scarcity of SD in-situ data in Svalbard, it is generally a challenge to quantify the accuracy of the products. For the similar observation periods and acquisition times, the interferometric coherence time series will be documented. As an estimate of the phase standard deviation, coherence values give a relative measure of stability/certainty (Balmer & Hartl, 1998) that can be used to weight the measurements in the model.

3.1.5 Product attributes

SD products	Unit	Property	Values provided	Product string
Seasonal SD time series	mm / unitless	SBAS-based displacement time series (2017–2021)	Displacement progression relative to first seasonal acquisition, / coherence time series	SSD
Multi-seasonal SD maps	mm	Averaged maximal displacement of the seasons (2017–2021)	Mean, median and standard deviation of the maximal seasonal	MSD

			displacement (2017–2021), averaged coherence	

3.1.6 Data documentation and dissemination

The datasets will be published on PANGAEA (targeting permafrost community) at the end of the project (Q4 2024).

3.2 Ground temperature at a certain depth (GTD) and active layer thickness (ALT)

3.2.1 Product description

This product includes the ECV state variables ground temperature and active layer thickness derived from a thermal model driven by land surface temperature data. The ground temperature at a certain depth (maximum 5 m) (**GTD**) and the active layer thickness (**ALT**) will be provided **at two spatial scales**:

- **Proof-of-concept products at the local scale**: One-dimensional point-scale simulations will be performed at selected locations with available land surface temperature (LST) measurements from in-situ instrumentation. The results will be directly comparable with GTD and ALT from permafrost monitoring in boreholes. The model will be run before and after assimilation of the InSAR SD products to compare the performance.
- **Experimental products at the regional scale**: For the flat lowlands of the ADV, NYA and KL study areas (see Section 2), the model will be driven by ERA-5 reanalysis data. The model will be run before and after the assimilation of InSAR SD products. While the initial Permafrost_cci product has a 1 km resolution, the results after the SD assimilations will be at the higher resolution of the InSAR SD products (40–100 m) (see Section 3.1).

Considering the period for which we will process the SD products (see Section 3.1), we will essentially focus on the similar years (2017–2021) for testing the assimilation procedure and generating GTD and ALT. The model spin-up largely follows the accelerated spin-up procedure described in the Section 3.1.4 of Westermann et al. (2022). Subsurface properties constrained by assimilation of the SD products are also expected to lead to an improved performance in the earlier years.

3.2.2 Temporal resolution

- **At the local scale** (one-dimensional point-scale simulations), the products will have a daily resolution.
- **At the regional scale** (ADV, NYA and KL study areas, see Section 2), we will provide products with one-year temporal resolution, which corresponds to average mean annual ground temperature, as well as the maximum depth of seasonal thaw, which corresponds to the active layer thickness.

3.2.3 Spatial resolution

The spatial resolution of the initial Permafrost_cci products is linked to the best available resolution of the input sensor. Here, the spatial resolution is limited to 1 km, which is the spatial resolution of remotely sensed LST. However, an ensemble-based modelling of subpixel variability is applied, i.e. different ensemble members represent different ground stratigraphies and snow depths found within the 1 km pixels. This is required for computation of permafrost and talik fractions. Considering the specific objective of assimilating InSAR products within the model, the regional GTD and ALT products of the IceInSAR Option 7 will be downscaled based on the higher resolution InSAR-based SD products. The variability of the results within a 1 km grid of the initial Permafrost_cci products (and the resulting computed permafrost and talik fractions) will be compared with the results from the representation of subpixel variability based on ensemble-based modelling.

3.2.4 Product properties

ECV variable	Unit	Property	Values provided	Product string
Ground temperature at certain depth (maximum 5 m)	degree C	**At the local scale:** daily modelled temperature **At the regional scale:** annual average	Results before and after InSAR-based SD assimilation. **At the regional scale:** Median and standard deviation of the ensemble	GTD
Active layer thickness	m	**At the local scale:** daily thaw depth **At the regional scale:** annual maximum thaw depth		ALT

3.1.5 Product accuracy

With respect to the threshold user requirements documented in the URD [RD-1], the following accuracy is targeted in year 2/3 of phase 1:

- **Ground temperature:** 2.0 degrees C compared to GTN-P boreholes (URq_12).
- **Active layer thickness:** RMSE < 0.25 m for ALT < 1.0 m and RMSE < 0.5 m for ALT > 1.0 m (URq_13).

Product accuracy of the years 1 and 2 of the Permafrost_cci Phase 1 products are documented in the PVIR [RD-3] [RD-4]. The accuracy of the CRDP v3 (phase 1, year 3) [RD-5] demonstrates for Mean Annual Ground Temperature (MAGT) time series from 1997 to 2019 across all depths an absolute bias of 1.58 °C, a mean bias of 0.98 °C and an RMSE of 1.93 °C for the whole range of validation data. Considering only permafrost measurement borehole sites with an MAGT < 1 °C, we get an absolute bias of 1.46 °C, a mean bias of -0.01 °C and an RMSE of 1.87 °C. Active layer thickness of the CRDP v3 (phase 1, year 3) is characterized by an absolute bias of 30 cm, a mean bias of -1.08 cm and an RMSE of 47 cm, when calculated for the bulk dataset. Results in Svalbard displays a positive bias attributed to the unrealistic landcover categorisation of this region. As a contribution to refine the documentation of the ground stratigraphy, InSAR-based SD products are expected to improve the modelled results in Svalbard.

3.1.6 Data exploitation and dissemination

The results will provide new findings valuable for the discussion of the Permafrost_cci data quality and will be used in the Product Validation and Intercomparison Report (PVIR) of the Phase 2.

The datasets will be published on PANGAEA () at the end of the project (Q4 2024).

4 PRODUCT FORMATS

4.1 Surface displacement (SD)

4.1.1 Product projection system

The Coordinate Reference System (CRS) used for the IceInSAR Option 7 in Svalbard will be projected in Transverse Mercator UTM 33N based on the World Geodetic System 1984 (WGS 1984) reference ellipsoid. The coordinates are specified in meters. Information on product projection, ellipsoid and pixel size will be included in the NetCDF.

4.1.2 File formats

All datasets are provided in NetCDF format.

4.1.3 Product file naming conventions

The files for each product type are named as follows:

ESACCI-<CCI Project>-<Processing Level>-<Data Type>-<Product String>[-<Additional Segregator>]-<Start Date>-<End Date>-fv<File version>.nc

<CCI Project>
PERMAFROST for permafrost_cci

<Processing Level>
L3 for Level 3 (SSD).

L4 for Level 4 (MSD)

<Data Type>
SSD: Seasonal surface displacement time series.
MSD: Multi-seasonal surface displacement maps.

<Product String>
This should be structured as: **<Source>_<Algorithm>**:
- **<Source>**: SENTINEL-1: SAR images from Sentinel-1.
- **<Algorithm>**: INSAR: Products processed with an INSAR algorithm.

<Additional Segregator>
This should be structured as: **AREA<Area number>_<Subarea name>_<Layer type >**
- <**Area number**>: 9 for Nordenskiöld Land (Svalbard).
- <**Subarea name**>: ADV, NYA or KL.
- **<Layer type >: DISP or COH**

<Start Date> and <End Date>
The identifying dates for the dataset:
Format is YYYYMMDD, where YYYY is the four-digit year, MM is the two-digit month from 01 to 12 and DD is the two-digit day of the month from 01 to 31. Annual or multi-annual products are represented with YYYY only.

fv<File Version>
File version number in the form n{1,}[.n{1,}] (two digits followed by a point and one or more digits).

Examples:
ESACCI-PERMAFROST-L3-SSD-SENTINEL1_INSAR-AREA9_NYA_DISP-2019-fv01.0.nc

4.1.4 File metadata

The following attributes are included in the NetCDF file:

Global Attribute	Content
title	ESA CCI permafrost <parameter name>
institution	NORCE Norwegian Research Centre
source	<text>
history	YYYY-MM-DD HH:MM:SS
references	http://cci.esa.int/Permafrost [and publications]
tracking_id	<xxxxxxxx-yyyy-zzzz-nnnn-mmmmmmmmmmmm> a UUID (Universal Unique Identifier) value
Conventions	CF-1.9
product_version	<number>
summary	<text>
keywords	<text>
id	<filename>
naming authority	no.norce
keywords_vocabulary	NASA Global Change Master Directory (GCMD) Science Keywords
cdm_data_type	Grid
comment	These data were produced at ESACCI as part of the ESA Permafrost CCI+ project Contract No 4000123681/18/I-NB
date_created	<file creation date>
creator_name	NORCE Norwegian Research Centre
creator_url	https://www.norceresearch.no
project	Climate Change Initiative - European Space Agency
geospatial_lat_min	30
geospatial_lat_max	90
geospatial_lon_min	-180
geospatial_lon_max	180
geospatial_vertical_min	0.0

Global Attribute	Content
geospatial_vertical_max	0.0
time_coverage_start	YYYYMMDDTHHMMSSZ
time_coverage_end	YYYYMMDDTHHMMSSZ
time_coverage_duration	P<number of years>Y
time_coverage_resolution	P<number><unit>
standard_name_vocabulary	CF Standard Name Table v73
license	ESA CCI Data Policy: free and open access
platform	<name>
spatial_resolution	<number><
geospatial_lat_units	none
geospatial_lon_units	none
geospatial_lon_resolution	<number><
geospatial_lat_resolution	<number><
key_variables	<name>
format_version	CCI Data Standards v2.2

4.2 Ground temperature at a certain depth (GTD) and active layer thickness (ALT)

4.2.1 Product projection system

The Coordinate Reference System (CRS) used for the IceInSAR Option 7 in Svalbard will be projected in Transverse Mercator UTM 33N based on the World Geodetic System 1984 (WGS 1984) reference ellipsoid. The coordinates are specified in meters. Information on product projection, ellipsoid and pixel size will be included in the NetCDF.

4.2.2 File formats

All datasets are provided in NetCDF format.

4.2.3 Product file naming conventions

The files for each product type are named as follows:

ESACCI-<CCI Project>-<Processing Level>-<Data Type>-<Product String>[-<Additional Segregator>]-<Start Date>-<End Date>-fv<File version>.nc

<CCI Project>
PERMAFROST for permafrost_cci

<Processing Level>

L4 for Level 4.

<Data Type>
GTD: ground temperature at a certain depth. ALT: active layer thickness.

<Product String>
This should be structured as: **<Source>_<Algorithm>**:

<Source>: MODIS: Land surface temperature from the Moderate Resolution Imaging Spectroradiometer instrument. INSITU: Land surface temperature from in-situ loggers.
<Algorithm>: CRYOGRID: Products processed with a CRYOGRID algorithm.

<Additional Segregator>
This should be structured as: **AREA<Area number>_<Subarea name>_<Layer type>_<Model constrain>**

<**Area number**>: 9 for Nordenskiöld Land (Svalbard).
<**Subarea name**>: ADV, NYA or KL.
<**Layer type**>: PP: permafrost parameter regional products. PT: permafrost parameter point-scale products (one-dimensional simulations).
<**Model constrain**>: INIT: initial model (before InSAR assimilation). CONS: SD-constrained model (after InSAR assimilation).

<Start Date> and <End Date>
The identifying dates for the dataset:
Format is YYYYMMDD, where YYYY is the four-digit year, MM is the two-digit month from 01 to 12 and DD is the two-digit day of the month from 01 to 31. Annual or multi-annual products are represented with YYYY only.

fv<File Version>
File version number in the form n{1,}[.n{1,}] (two digits followed by a point and one or more digits).

Examples:
ESACCI-PERMAFROST-L4-GTD-MODIS_CRYOGRID-AREA9_ADV_PT_CONS-2017-fv01.0.nc

4.1.4 File meta data - NetCDF

The following attributes are included in the NetCDF file:

Global Attribute	Content
title	ESA CCI permafrost <parameter name>
institution	University of Oslo
source	<text>
history	YYYY-MM-DD HH:MM:SS
references	http://cci.esa.int/Permafrost [and publications]
tracking_id	<xxxxxxxx-yyyy-zzzz-nnnn-mmmmmmmmmmmm> a UUID (Universal Unique Identifier) value
Conventions	CF-1.9
product_version	<number>

Global Attribute	Content
summary	<text>
keywords	<text>
id	<filename>
naming authority	no.uio
keywords_vocabulary	NASA Global Change Master Directory (GCMD) Science Keywords
cdm_data_type	Grid
comment	These data were produced at ESACCI as part of the ESA Permafrost CCI+ project Contract No 4000123681/18/I-NB
date_created	<file creation date>
creator_name	University of Oslo
creator_url	https://www.uio.no/english
project	Climate Change Initiative - European Space Agency
geospatial_lat_min	30
geospatial_lat_max	90
geospatial_lon_min	-180
geospatial_lon_max	180
geospatial_vertical_min	0.0
geospatial_vertical_max	0.0
time_coverage_start	YYYYMMDDTHHMMSSZ
time_coverage_end	YYYYMMDDTHHMMSSZ
time_coverage_duration	P<number of years>Y
time_coverage_resolution	P<number><unit>
standard_name_vocabulary	CF Standard Name Table v73
license	ESA CCI Data Policy: free and open access
platform	<name>
spatial_resolution	<number><
geospatial_lat_units	none
geospatial_lon_units	none
geospatial_lon_resolution	<number><
geospatial_lat_resolution	<number><

Global Attribute	Content
key_variables	<name>
format_version	CCI Data Standards v2.2

5 REFERENCES

5.1 Bibliography

Balmer & Hartl, 1998 Bamler, R., & Hartl, P. (1998). Synthetic aperture radar interferometry. *Inverse problems*, *14*(4), R1. https://doi.org/10.1088/0266-5611/14/4/001.

Bartsch, A., Leibman, M., Strozzi, T., Khomutov, A., Widhalm, B., Babkina, E., Mullanurov, D., Ermokhina, K., Kroisleitner, C. & Bergstedt, H. (2019). Seasonal progression of ground displacement identified with satellite radar interferometry and the impact of unusually warm conditions on permafrost at the Yamal Peninsula in 2016. *Remote Sensing*, *11*(16), 1865. https://doi.org/10.3390/rs11161865.

Berardino, P., Fornaro, G., Lanari, R., & Sansosti, E. (2002). A new algorithm for surface deformation monitoring based on small baseline differential SAR interferograms. *IEEE Transactions on geoscience and remote sensing*, *40*(11), 2375–2383. https://doi.org/10.1109/TGRS.2002.803792.

Boike, J., Roth, K., & Ippisch, O. (2003). Seasonal snow cover on frozen ground: Energy balance calculations of a permafrost site near Ny-Ålesund, Spitsbergen. *Journal of Geophysical Research: Atmospheres*, *108*(D2), ALT-4. https://doi.org/10.1029/2001JD000939.

Boike, J., Juszak, I., Lange, S., Chadburn, S., Burke, E., Overduin, P. P., ... & Westermann, S. (2018). A 20-year record (1998–2017) of permafrost, active layer and meteorological conditions at a high Arctic permafrost research site (Bayelva, Spitsbergen). *Earth System Science Data*, *10*(1), 355–390. https://doi.org/10.5194/tc-4-475-2010.

Cable, S., Elberling, B., & Kroon, A. (2018). Holocene permafrost history and cryostratigraphy in the High-Arctic Adventdalen Valley, central Svalbard. *Boreas*, *47*(2), 423–442. https://doi.org/10.1111/bor.12286.

Christiansen, H. H., Etzelmüller, B., Isaksen, K., Juliussen, H., Farbrot, H., Humlum, O., ... & Ødegård, R. S. (2010). The thermal state of permafrost in the nordic area during the international polar year 2007–2009. *Permafrost and Periglacial Processes*, *21*(2), 156–181. https://doi.org/10.1002/ppp.687.

Christiansen, H. H., Gilbert, G. L., Neumann, U., Demidov, N., Guglielmin, M., Isaksen, K., ... & Boike, J. (2021). Ground ice content, drilling methods and equipment and permafrost dynamics in Svalbard 2016–2019 (PermaSval). *SESS report 2020 - The State of Environmental Science in Svalbard - Annual report*, *3*.

Eckerstorfer, M., Malnes, E., & Christiansen, H. H. (2017). Freeze/thaw conditions at periglacial landforms in Kapp Linné, Svalbard, investigated using field observations, in situ, and radar satellite monitoring. *Geomorphology*, *293*, 433–447. https://doi.org/10.1016/j.geomorph.2017.02.010.

Emardson, T. R., Simons, M., & Webb, F. H. (2003). Neutral atmospheric delay in interferometric synthetic aperture radar applications: Statistical description and mitigation. *Journal of Geophysical Research: Solid Earth*, *108*(B5). https://doi.org/10.1029/2002JB001781.

Hanssen, R. F. (2001). *Radar interferometry: data interpretation and error analysis* (Vol. 2). Springer Science & Business Media.

Gilbert, G. L., O'Neill, H. B., Nemec, W., Thiel, C., Christiansen, H. H., & Buylaert, J. P. (2018). Late Quaternary sedimentation and permafrost development in a Svalbard fjord-valley, Norwegian high Arctic. *Sedimentology*, *65*(7), 2531–2558. https://doi.org/10.1111/sed.12476.

Hanssen-Bauer, I., Førland, E.J., Hisdal, H., Mayer, S., Dandé, A.B. & Sorteberg, A. (2019). *Climate in Svalbard 2100*; NCCS report no. 1/2019. Norwegian Centre for Climate Services (NCCS). Norwegian Environment Agency (Miljødirektoratet): Trondheim, Norway.

Hjelle, A. (1999). *Geological Map of Svalbard 1: 100,000: Sheet A7G Kongsfjorden*; Norwegian Polar Institute: Tromsø, Norway.

Landvik, J.Y. & Salvigsen, O. (1987). The late Weichselian and Holocene shoreline displacement on the West-Central coast of Svalbard. *Polar Res.* **1987**, *5*, 29–44. https://doi.org/10.1111/j.1751-8369.1987.tb00353.x.

Major H.; Haremo, P.; Dallmann, W.K.; Andresen, A.; Salvigsen, O. (2001). *Geological Map of Svalbard 1: 100,000, Sheet C9G Adventdalen*; Norwegian Polar Institute: Tromsø, Norway.

Miccadei, E., Piacentini, T., & Berti, C. (2016). Geomorphological features of the Kongsfjorden area: Ny-Ålesund, Blomstrandøya (NW Svalbard, Norway). *Rendiconti Lincei*, *27*(1), 217–228. https://doi.org/10.1007/s12210-016-0537-3.

Peel, M.C.; Finlayson, B.L.; McMahon, T.A. (2007) Updated world map of the Köppen-Geiger climate classification. *Hydrol. Earth Syst. Sci.*, *11*, 1633–1644. https://doi.org/10.5194/hess-11-1633-2007.

Retelle, M., Christiansen, H., Hodson, A., Nikulina, A., Osuch, M., Poleshuk, K., ... & Wawrzyniak, T. (2019). Environmental monitoring in the Kapp Linne-Gronfjorden Region (KLEO). *The State of Environmental Science in Svalbard*.

Rouyet, L., Lauknes, T. R., Christiansen, H. H., Strand, S. M., & Larsen, Y. (2019). Seasonal dynamics of a permafrost landscape, Adventdalen, Svalbard, investigated by InSAR. *Remote Sensing of Environment*, *231*, 111236, https://doi.org/10.1016/j.rse.2019.111236.

Rouyet, L., Liu, L., Strand, S. M., Christiansen, H. H., Lauknes, T. R., & Larsen, Y. (2021). Seasonal InSAR Displacements Documenting the Active Layer Freeze and Thaw Progression in Central-Western Spitsbergen, Svalbard. *Remote Sensing*, *13*(15), 2977. https://doi.org/10.3390/rs13152977.

Tolgensbakk, J., Sørbel, L., Høgard, K. (2001). *Geomorphological and Quaternary Geological Map of Svalbard 1: 100,000. Sheet C9Q Adventdalen. Temakart 31*; Norwegian Polar Institute: Tromsø, Norway, 2001.

Westermann, S., Wollschläger, U., & Boike, J. (2010). Monitoring of active layer dynamics at a permafrost site on Svalbard using multi-channel ground-penetrating radar. *The Cryosphere*, *4*(4), 475–487. https://doi.org/10.5194/tc-4-475-2010

Westermann, S., Langer, M., & Boike, J. (2011). Spatial and temporal variations of summer surface temperatures of high-arctic tundra on Svalbard—Implications for MODIS LST based permafrost monitoring. *Remote Sensing of Environment*, *115*(3), 908–922. https://doi.org/10.1016/j.rse.2010.11.018.

Westermann, S., Ingeman-Nielsen, T., Scheer, J., Aalstad, K., Aga, J., Chaudhary, N., ... & Langer, M. (2022, in review). The CryoGrid community model (version 1.0) – a multi-physics toolbox for climate-driven simulations in the terrestrial cryosphere. *Geoscientific Model Development Discussion* [preprint]. https://doi.org/10.5194/gmd-2022-127.

Zwieback, S., & Meyer, F. J. (2021). Top-of-permafrost ground ice indicated by remotely sensed late-season subsidence. *The Cryosphere*, *15*(4), 2041–2055. https://doi.org/10.5194/tc-15-2041-2021.

Åkerman, H.J. (2005) Relations between slow slope processes and active-layer thickness 1972–2002, Kapp Linné, Svalbard. *Nor. Geogr. Tidsskr. Nor. J. Geogr.* **2005**, *59*, 116–128, https://doi.org/10.1080/00291950510038386.

5.2 Acronyms

AD	Applicable Document
ADV	Adventdalen
ALT	Active Layer Thickness
APS	Atmospheric Phase Screen
B.GEOS	B.Geos GmbH
CCI	Climate Change Initiative
CRDP	Climate Research Data Package
CRS	Coordinate Reference System
ECV	Essential Climate Variable
EO	Earth Observation
ESA	European Space Agency
GAMMA	Gamma Remote Sensing AG
GCOS	Global Climate Observing System
GT	Ground Temperature
GTD	Ground Temperature at certain depth
GTN-P	Global Terrestrial Network for Permafrost
InSAR	Synthetic Aperture Radar Interferometry
IPA	International Permafrost Association
IPCC	Intergovernmental Panel on Climate Change
IW	Interferometric Wide
KL	Kapp Linné
LOS	Line-of-sight
LST	Land Surface Temperature
MAGT	Mean Annual Ground Temperature
MAGST	Mean Annual Ground Surface Temperature
MSD	Multi-seasonal Surface Displacement
NetCDF	Network Common Data Format
NORCE	Norwegian Research Centre
NYA	Ny-Ålesund
PFR	Permafrost extent (Fraction)
PFF	Permafrost-Free Fraction
PFT	Permafrost underlain by Talik
PVIR	Product Validation and Intercomparison Report
PSD	Product Specification Document

PSTG	Polar Space Task Group
PZO	Permafrost Zone
RD	Reference Document
RMSE	Root Mean Square Error
RS	Remote Sensing
SBAS	Small Baseline Subset
SAR	Synthetic Aperture Radar
SD	Surface Displacement
SSD	Seasonal Surface Displacement
SSI	Single Seasonal Interferograms
TSP	Thermal State of Permafrost
UIO	University of Oslo
URD	Users Requirement Document
URq	User Requirement
WGS 84	World Geodetic System 1984